TÜBİTAK

Turkish Journal of Chemistry

http://journals.tubitak.gov.tr/chem/

Research Article

Turk J Chem
(2017) 41: 793 – 801

doi:10.3906/kim-1611-17

The multiple effects of organoclay and solvent evaporation on hydrophobicity of composite surfaces

Hac Hasan YOLCU[1,2,*], **Ahmet GÜRSES**[3], **Rabah BOUKHERROUB**[2]
[1]Department of Chemistry, Faculty of Education, Kafkas University, Kars, Turkey
[2]Institut d'Electronique, de Microélectronique et de Nanotechnologie (IEMN), UMR CNRS 8520, Villeneuve d'Ascq, France
[3]Department of Chemistry, Kazım Karabekir Faculty of Education, Atatürk University, Erzurum, Turkey

Received: 10.11.2016 • **Accepted/Published Online:** 06.05.2017 • **Final Version:** 10.11.2017

Abstract: A superhydrophobic high-density polyethylene (HDPE)/organoclay composite material with a water-static contact angle of ∼162° and low hysteresis (7°) was prepared by a simple solution-intercalation technique. This one-step method consists of the insertion of organoclay, produced through cation exchange with cetyltrimethylammonium bromide (CTAB), in the polymer matrix at 120 °C in xylene. In this process, evaporation of the solvent and organoclay amount are key factors for the achievement of superhydrophobicity. We characterized composite material with X-ray diffraction (XRD), scanning electron microscopy (SEM), transmission electron microscopy (TEM), and contact angle measurements. The characterizations showed that the organoclay provides a place for the formation of small polymer aggregates and facilitates the evaporation of the organic solvent. The technique described here is simple and does not require any complicated process.

Key words: High-density polyethylene, organoclay, composite material, superhydrophobicity

1. Introduction

Recent advances in the preparation of superhydrophobic and self-cleaning materials have received a great deal of attention because of their potential industrial applications and their importance in fundamental research.[1,2] Superhydrophobic and self-cleaning surfaces with a high-static water-contact angle of 150° and low-contact angle hysteresis play an important role in technical applications ranging from microfluidics,[3] protection against marine fouling,[4] membrane distillation,[5] self-cleaning paints and textiles,[6] anti-icing surfaces,[7] and lab-on-chip devices.[3]

The wettability of solid surfaces is controlled by both the chemical composition and the geometrical microstructure of the surface. To obtain superhydrophobic surfaces, a cooperative effect of low-surface free-energy materials and micro-/nanostructures is required. Superhydrophobic surfaces with water-contact angles larger than 150° have been obtained by controlling the surface topography by various processing methods, such as anodic oxidation,[8] plasma treatment,[9] chemical vapor deposition,[10] spraying,[11] colloidal sediment,[12] and solvent evaporation.[13] The main effect of a topographic structure on super water repellency has been well simulated with Wenzel[14] and Cassie–Baxter[15] models. Both models have emphasized the geometrical structure of solid surfaces as an important factor in determining the wettability.

*Correspondence: yolcu.hasan@gmail.com

Organic/inorganic nanocomposites have attracted great interest because they often exhibit unusual properties.[16–18] Polymer composite materials are widely used systems to enhance environmental and thermal stability, for chemical resistance, as fire retardants, to promote recycling, and to reduce weight in various applications such as transportation vehicles, construction materials, electronics, and sporting goods. Generally, an inorganic material exhibits a low interaction with organic polymers. To overcome this hurdle and to improve the compatibility of the clay and the polymer, the use of organoclays as precursors to composite formation has been widely adopted.[17] To this end, the replacement of the inorganic exchange cations of the native clay by alkylammonium surfactants modifies the clay's surface properties from hydrophilic to hydrophobic and thus allows an easy processability of the clay and the hydrophobic polymer matrix.

The fabrication of superhydrophobic polymer-organoclay composite materials has been described in a few reports.[19,20] Bayer et al. reported on the preparation of rubber-toughened biopolymer/organoclay composite coatings with a highly water-repellent surface and strong adhesion to metal surfaces.[21] The same group also studied the temperature and humidity effects on the superhydrophobicity of polyurethane/organoclay composites.[20] They found that superhydrophobicity was maintained for a full temperature cycle of 20 °C to 3 °C in a low-humidity environment, while superhydrophobicity degradation was observed for high humidity during the warm-up cycle.[20]

In the present work, we report on the preparation of superhydrophobic high-density polyethylene (HDPE)/organoclay composites. The technique used here is simple, straightforward, and does not require a complicated process. It consists of the modification of the surface energy of the clay through cation exchange with CTAB and clay subsequent insertion into porous HDPE at 110 °C in xylene. Slow evaporation of the solvent at room temperature produced a HDPE/organoclay composite with high contact angles ($>160°$) and low-contact angle hysteresis ($<10°$) (Figure 1). Slow evaporation and lower drying temperatures increased the nucleation rate and pore formation.[22,23] While superhydrophobic low-density polyethylene (LDPE)[24] and HDPE[25] surfaces have been previously described, the preparation of superhydrophobic HDPE/organoclay composites, to the best of our knowledge, has not yet been reported on.

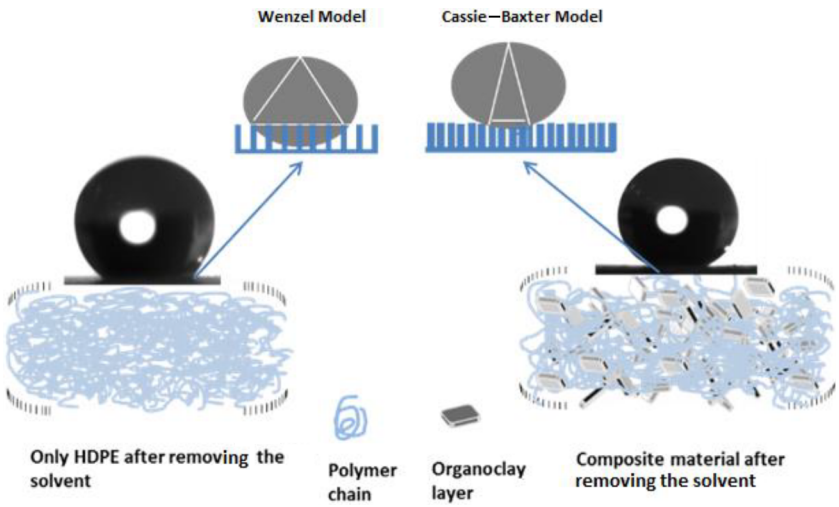

Figure 1. Schematic illustration of the preparation of superhydrophobic HDPE/organoclay surfaces.

2. Results and discussion

Figures 2a and 2b show XRD patterns of the HDPE and HDPE/organoclay composites at different clay concentrations. The XRD patterns of the composite with an organoclay concentration of 2.5 and 5 wt% show two diffraction peaks in a 2 θ range of 21–25°, corresponding to the (110) and (200) lattice planes of the HDPE, in accordance with previously published data.[26] Increasing the organoclay concentration to 10% in the composite did not cause any major difference in the XRD pattern, although there were no evident peaks in the clay (absence of the peak at 2 θ= 15°). The absence of the peaks from the clay is an indication that the clay layers were exfoliated or intercalated in the composite. An increase of the organoclay peak's intensity was observed for clay loadings of 15 wt%. The sharper peak in the XRD pattern of HDPE/organoclay can be attributed to the crystallization rate. Crystallization began in the clay-rich phase by the formation of crystal nuclei. The 2.5 wt% of organoclay TEM result also supports the XRD results (Figure 3). TEM images were presented to support the confirmation of the dispersion of organoclay in the polymer matrix. Dark lines correspond to the cross section of the organoclay layers and the gap between the two adjacent lines is the interlayer space.

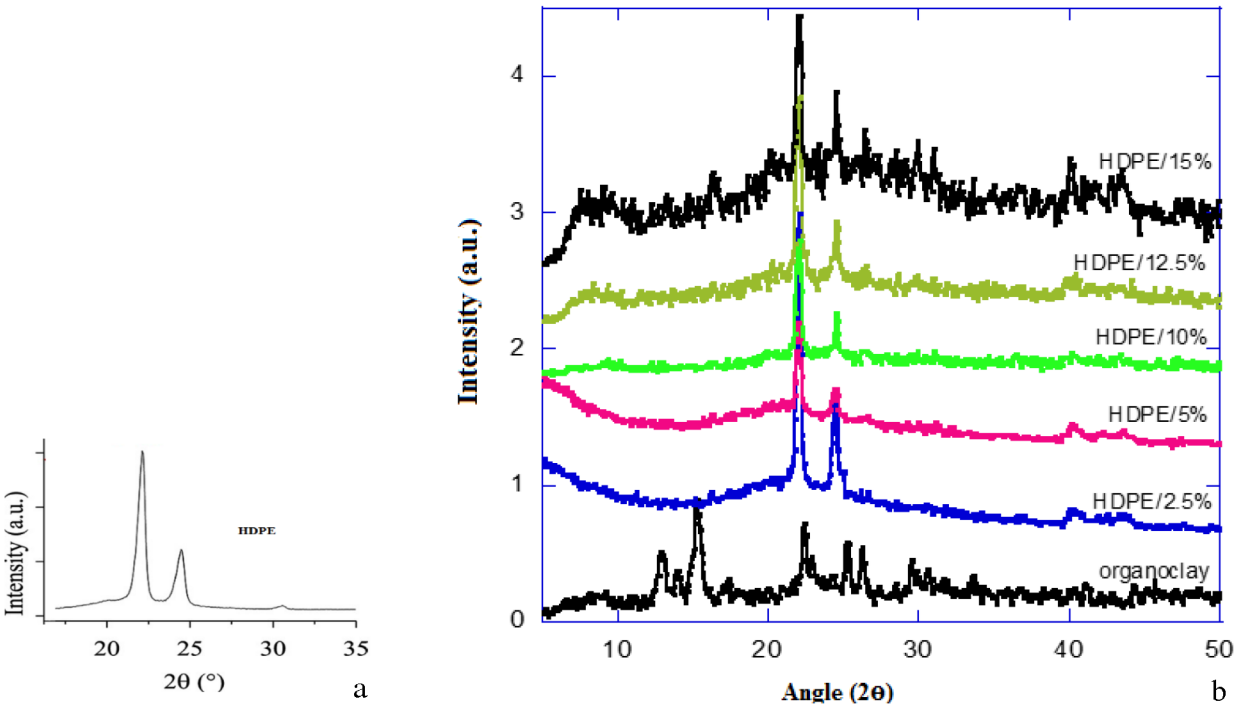

Figure 2. X-ray diffraction patterns of the a) HDPE and b) organoclay and HDPE/organoclay composites for different organoclay contents.

Modification of clay mineral surfaces through adsorption of organic surfactants has been studied extensively in the literature with emphasis on the preparation of clay-polymer composites with reinforced properties.[18] Although organoclays are mostly used as fillers in polymers to improve the mechanical, thermal, and sorption capacity of the resulting organoclay/polymer composites, there are only a few examples on the study of their wetting properties.[20]

We have used CTAB to modify the clay surface properties through cation exchange to match the wetting properties of the host polymer, HDPE. The water-contact angle of bulk HDPE was 97°. The CTAB-modified

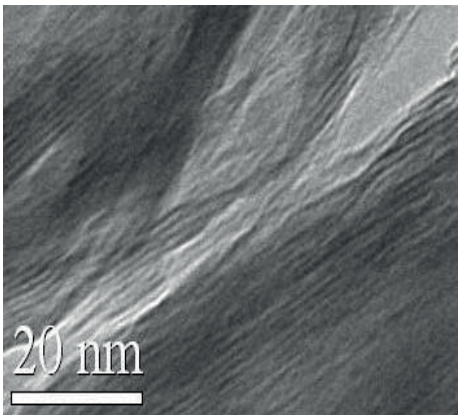

Figure 3. High-resolution TEM image of 5 wt% of organoclay.

clay displayed a water-contact angle of 52°. This is higher than the water-contact angle measured in the unmodified clay (28°). The observed increase in contact angle could be attributed to CTAB hydrophobic long-chain hydrocarbon. The zeta potential of the initial clay was –26.4 mV. After CTAB modification, the zeta potential increased to +9.6 mV, suggesting cation exchange with the clay.

We prepared polymer and polymer/organoclay composite films on glass slides through solution casting in xylene, following the procedure developed by Erbil et al. for isotactic polypropylene.[23] Based on the pioneering work by Erbil et al. and that reported by Yuan et al,[25] who showed that higher water-contact angles were achieved by lowering the drying temperature, we performed the drying step at room temperature. Figure 4 shows SEM images of HDPE and HDPE/organoclay composites processed in xylene at 120 °C after drying at room temperature for 1 day. In the absence of organoclay, the glass slide was coated homogeneously with a flake-like HDPE film without obvious pore formation. Introduction of organoclay into the polymer matrix induced pore formation up to 2.5 wt% of organoclay. The preferred pore size and amount for the hydrophobicity were obtained between 5 and 15 wt% organoclay amounts. Organoclay provides a smaller aggregate in the structure. The contact angle hysteresis decreases change the surface roughness model could be from Wenzel to the Cassie–Baxter model (Figure 1). There is also evidence for crystallite formation in the polymer-rich matrix. Above this concentration, pore filling occurred (Figure 4).

We have investigated the effect of the organoclay concentration on the superhydrophobic properties of the HDPE/organoclay composites. In all experiments, the drying was performed at room temperature for 1 day. In the absence of organoclay, the HDPE film displayed a water-contact angle of 150° and a contact-angle hysteresis of 14° (Figures 5a and 5b).

This value is comparable to that measured on an LDPE surface (151°) at a solvent evaporation temperature of 30 °C,[24] but slightly lower than that reported on isotactile polypropylene (155°, drying temperature of 30 °C)[27] and higher than on HDPE/xylene dried at 20 °C (142°).[25] Intercalation of organoclay in the polymer matrix led to an increase in the contact angle to about 160° with a decrease in the hysteresis to 7°. This slight increase in the contact angle and the decrease in the hysteresis are most likely due to the change in the film morphology through pore formation. The water-contact angle increased to 162° upon insertion of 10 wt% of organoclay and then decreased to 158° for 15% of organoclay. The contact-angle hysteresis on the other hand increased from 9 to 13° for organoclay concentrations of 10 wt% and 15 wt%, respectively. This behavior is most likely due to the morphological changes of the HDPE/organoclay composite film upon

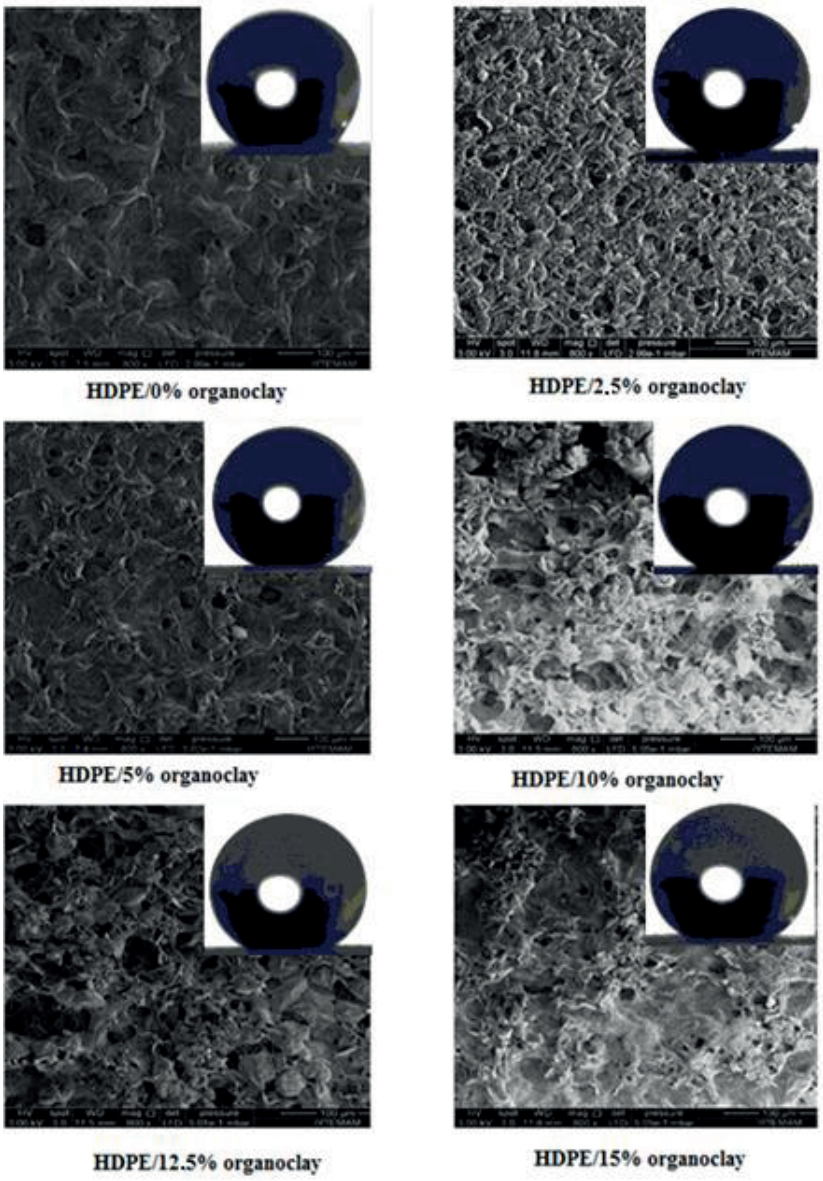

Figure 4. SEM images of HDPE/organoclay composites for different organoclay contents.

increasing organoclay concentration. The result is in accordance with the SEM observation, suggesting pore filling for 15 wt% organoclay.

To improve the water-contact angle and decrease the contact-angle hysteresis, Yuan et al. added ethanol in the HDPE solution and performed the drying process at 5 °C in a humid atmosphere (relative humidity between 60% and 75%). Under these conditions, a contact of 160° and a sliding angle of 2° were measured on the porous HDPE surface.[25] Ethanol is a nonsolvent for HDPE; its addition in the polymer solution decreases HDPE solubility and thus induces the formation of more uniform HDPE aggregates during the solidification process.[25] A similar approach has been proposed in earlier work by Erbil et al.[23] They showed that the use of nonsolvents (such as methyl ethyl ketone, ethanol, cyclohexanone, and isopropyl alcohol) in conjunction with

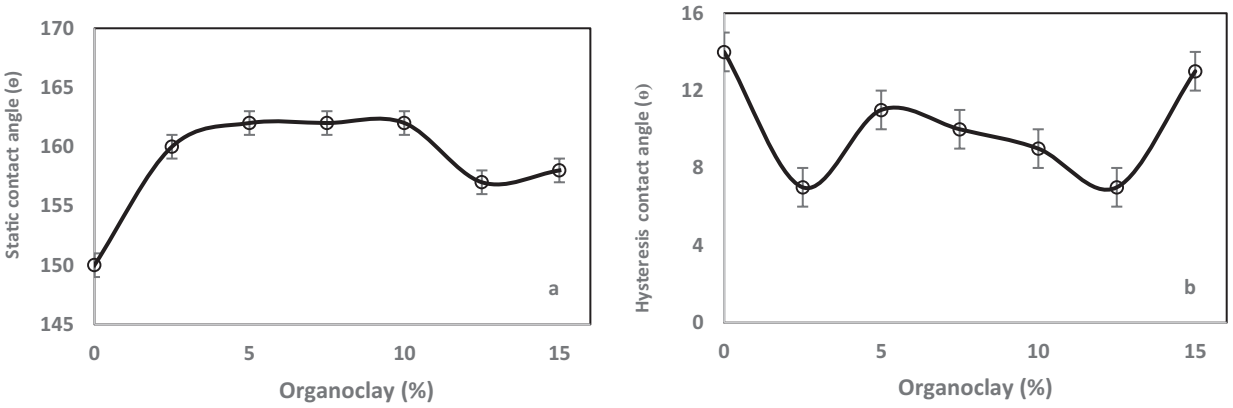

Figure 5. a) Water static contact angle and b) contact angle hysteresis as a function of organoclay content.

xylene favors the formation of small aggregates through phase separation, increases the nucleation rate, and decreases the crystallization time. The same strategy has been adopted by Lu et al. for the preparation of superhydrophobic LDPE surfaces. They demonstrated that the addition of cyclohexanone in the polymer/xylene solution, followed by solvent evaporation at room temperature under vacuum, produced a surface with a contact angle of 173° and a sliding angle of 2°. They attributed the improvement in the contact angle to an increase in the crystallization time and nucleation rate.[23,24] In the present work, we think that the organoclay serves all these purposes, i.e. the organoclay provides a place for the formation of small polymer aggregates, facilitates the evaporation of the organic solvent, and decreases the crystallization time. Indeed, from the SEM imaging, it becomes clear that polymer phase separation takes place upon addition of organoclay (2.5% to 12.5%) in the HDPE/xylene solution. This induces polymer aggregation and pore formation. However, an increase in the organoclay concentration to 15 wt % causes pore filling, leading to a slight contact angle decrease and a sliding angle increase (Figures 5a and 5b).

3. Conclusion

We successfully prepared superhydrophobic HDPE/organoclay composite surfaces by a one-step process. The surface properties of the clay were controlled through adsorption of a surfactant, CTAB. The modification of the clay with CTAB allowed its compatibility with the hydrophobic polymer. Under optimal conditions, the addition of the organoclay to the HDPE/xylene solution provided surfaces with water contact angle as high as 162° and a sliding angle of 7° upon solvent evaporation at room temperature under ambient atmosphere. Because of its simplicity, this technique paves the way for the fabrication of a wide range of polymer/organoclay composites with enhanced properties and superhydrophobicity.

4. Experimental

4.1. Material

The natural clay sample was collected from the Erzurum region in Turkey and consisted of mineralogically mixed clay and nonclay minerals. The sample consisted of smectite (26%), chlorite (20%), illite (17%), and kaolinite (14%) (clay minerals) as well as analcime (11%), calcite (7%), quartz (3%), and feldspar (3%) (nonclay minerals). The CTAB-modified clay was prepared according to a previously published procedure on the preparation of surfactant modified montmorillonite.[28,29] The cation exchange capacity (CEC) of the clay was determined by

the methylene blue test (ANSI/ASTM C837-76). The results are given in Table 1. The chemical composition of the clay sample was determined by Rigaku RIX-3000 X-ray fluorescence spectrometry (Rigaku Corporation, Tokyo, Japan) and the results are presented in Table 2. High-density polyethylene (HDPE, $M_w \sim 125{,}000$), low density polyethylene and CTAB, xylene, and glass slides were supplied by Merck. Deionized water was obtained from a Milli-Q plus system (Millipore). The glass slides were cleaned several times with acetone and deionized water and then dried with nitrogen gas.

Table 1. Some physical properties of the clay sample.

CEC* [meq /100 g]	d* [g/cm^3]	OMC* [%]	Liquid limit W_L, [%]	a* [m^2/g]
48.9	2.61	5.10	102.00	64.20

*(CEC) Cation exchange capacity, (d) specific gravity, (OMC) organic matter content, (a) specific surface area.

Table 2. Chemical composition of the clay sample (%).

SiO_2	Al_2O_3	CaO	MgO	Fe_2O_3
45.12	13.70	7.48	7.29	5.63
K_2O	Na_2O	TiO_2	SO_3	P_2O_5
2.62	2.37	0.53	0.44	0.25

4.2. Preparation of CTAB-modified organoclays

The synthesis of CTAB modified clays was performed as follows: 2 g of clay was dispersed in deionized water and stirred for 10 h at stirring speed of 200–250 rpm to swell and to form a homogeneous solution. To this solution, an excess of CTAB (240 mg/L) was added. The resulting mixture was stirred for 1 h and then stirring was stopped. The CTAB-modified clay was filtered, washed with deionized water several times to remove excess salts, dried at 90 °C, ground, and sieved.

4.3. Preparation of HDPE hydrophobic surfaces

First 0.2 mg of HDPE was dissolved slowly in 5 mL of xylene at 110 °C to form a homogeneous solution. The resulting PE solution was then poured onto a cleaned glass slide and left at room temperature for 1 day for crystallization and evaporation.

4.4. Preparation of HDPE/organoclay superhydrophobic surfaces

In this study, a cationic surfactant, cetyltrimethylammonium bromide (CTAB), also known as hexadecyltrimethylammonium bromide, was used as an opposite charged surface active agent to produce a neutral organoclay sample.

For the composite material, a homogeneous solution was prepared by dissolving 0.2 mg of HDPE solution in 5 mL of xylene at 110 °C. Swollen organoclay (2.5, 5, 10, 12.5, or 15 wt%) in 5 mL of xylene was inserted in the polymer solution at 120 °C and the mixture was kept under stirring for 30 min at this temperature. The resulting gel was poured onto a glass slide and left at room temperature for 1 day for crystallization and evaporation.

4.5. Characterization

4.5.1. X-ray diffraction (XRD)

XRD measurements of the organoclay and composite materials samples were performed using Rigaku 2200 D/max (Rigaku Corporation, Tokyo, Japan) powder diffractometer equipment with a Cu Kα radiation (λ = 1.5418 Å) source at 30 kV, 10 mA, and at a scan rate of 2° in min unit.

4.5.2. Scanning electron microscopy (SEM)

SEM images were obtained using a field emission scanning electron microscope (Philips XL 30S FEG FEI Quanta 250 FEG, 3.00 kV).

4.5.3. Wetting properties

Water static contact angles were measured using 5 μL of distilled water. We used a remote-computer controlled goniometer system (CAM-101 optical contact angle analyzer, KSV Instruments, Finland). Each measurement was repeated four times and five frames, which were taken at the rate of 1 frame/s, were analyzed. The accuracy is $\pm 1°$. All measurements were made in ambient atmosphere at room temperature. During the measurement of advancing contact angle, a drop of deionized water, with a diameter of $\sim$5 μm, was formed at the tip of the needle and attached to the sample. The size of the droplet was increased until the base of the drop expanded on the sample surface and the advancing contact angle was measured several seconds after the size of the drop base stopped expansion. After 3–4 measurements of advancing contact angle were completed, the size of the water drop was reduced, until its base contracted, and the receding contact angle was measured. Contact angle hysteresis was calculated from the difference between the advancing contact angle and the receding contact angle.

4.5.4. Transmission electron microscopy (TEM)

Composite structures were studied by transmission electron microscopy (JEOL JEM 2100-F) with an accelerating voltage of 200 kV.

4.5.5. Zeta potential measurements

Zeta potential of the clay and CTAB-modified clay solutions in deionized water was measured using a Zetasizer Nano ZS (Malvern Instruments) instrument in 1731 scattering geometry. The reported values are averaged over 3 measurements, performed at 25 °C.

Acknowledgements

HY thanks the Council of Higher Education (Turkey) and Kafkas University, under project (2015–FM-76) for financial support. RB acknowledges financial support from the Centre National de la Recherche Scientifique (CNRS) and the Nord-Pas-de Calais region. We would like to thank the Civil Engineering Department of Atatürk University for providing the clay.

References

1. Zhang, L.; Zhao, N.; Xu, J. *J. Adhes. Sci. Technol.* **2014**, *28*, 769-790.
2. Zhang, P.; Lv, F. Y. A. *Energy.* **2015**, *82*, 1068-1087.
3. Gogolides, E.; Ellinas, K.; Tserepi, A. *Microelectron. Eng.* **2015**, *132*, 132-155.

4. Genzer, J.; Efimenko, K. *Biofouling* **2006**, *22*, 339-360.
5. Warsinger, D. M.; Servi, A.; Van Belleghem, S.; Gonzalez, J.; Swaminathan, J.; Kharraz, J.; Chung, H. W.; Arafat, H. A.; Gleason, K. K.; Lienhard V, J. H. *J. Memb. Sci.* **2016**, *505*, 241-252.
6. Rivero, P. J.; Urrutia, A.; Goicoechea, J.; Arregui, F. J. *Nanoscale Res. Lett.* **2015**, *10*, 505.
7. Lv, J.; Song, Y.; Jiang, L.; Wang, J. *ACS Nano.* **2014**, *8*, 3152-3169.
8. Qian, B.; Shen, Z. *Langmuir* **2005**, *21*, 9007-9009.
9. Han, D.; Steckl, A. *Langmuir* **2009**, *25*, 9454-9462.
10. Gupta, R. K.; Kumar, P.; Yadav, V.; Arora, S.; Singh, D. P.; Joshi, S. K.; Chawla, A. K.; Biswas. *Curr. Nanosci.* **2016**, *12*, 429-447.
11. Ogihara, H. *J. Vac. Soc. Japan* **2015**, *58*, 431-435.
12. Li, Y.; Huang, X.; Heo, S.; Li, C.; Choi, Y.; Cai, W. *Langmuir* **2007**, *23*, 2169-2174.
13. Erbil, H. Y. *Adv. Colloid Interface Sci.* **2012**, *170*, 67-86.
14. Wenzel, R. N. *Ind. Eng. Chem.* **1936**, *28*, 988-994.
15. Cassie, A.; Baxter, S. *Trans. Faraday Soc.* **1944**, *40*, 546-551.
16. Paul, D. R.; Robeson, L. M. *Polym. Nanocomposites* **2008**, *49*, 3187-3204.
17. Yalçınkaya, S. E.; Yıldız, N.; Saçak, M.; Çalımlı, A. *Turk. J. Chem.* **2010**, *34*, 581-592.
18. Delibaş, A.; Alparslan, M. *Turk. J. Chem.* **2015**, *39*, 630-638.
19. Fukushima, K.; Camino, G. *Polym. Nanocomposites* **2016**, 287-328.
20. Bayer, I.; Steele, A.; Martorana, P.; Loth, E. *Appl. Surf. Sci.* **2010**, *3*, 823-826.
21. Bayer, I.; Brown, A.; Steele, A.; Loth, E. *Appl. Phys. Express.* **2009**, *2*, 125001-125003.
22. Boinovich, L.; Emelyanenko, A. M.; Korolev, V. V; Pashinin, A. S. *Langmuir* **2014**, *30*, 1659-1668.
23. Erbil, H.; Demirel, A.; Avcı, Y.; Mert, O. *Science* **2003**, *299*, 1377-1380.
24. Lu, X.; Zhang, C.; Han, Y. *Macromol. Rapid Commun.* **2004**, *25*, 1606-1610.
25. Yuan, Z.; Chen, H.; Tang, J.; Zhao, D. *J. Appl. Polym.* **2009**, *113*, 126-1632.
26. Furukawa, T.; Sato, H.; Kita, Y.; Matsukawa, K.; Yamaguchi, H.; Ochiai, S.; Siesler, H. W.; Ozaki, Y. *Polym. J.* **2006**, *38*, 1127-1136.
27. Orkan Uçar, I.; Erbil, H. Y. *Turk. J. Chem.* **2013**, *37*, 643-674.
28. Acikyildiz, M.; Gurses, A.; Yolcu, H. H. *Acta Phys. Pol. A* **2015**, *127*, 1156-1160.
29. Kıranşan, M.; Soltani, R. D. C.; Hassani, A.; Karaca, S.; Khataee, A. *J. Taiwan Inst. Chem. Eng.* **2014**, *45*, 2565-2577.